European Heart Journal Supplements (2020) **22** (Supplement C), C15–C25
The Heart of the Matter
doi:10.1093/eurheartj/suaa006

Are we curing one evil with another? A translational approach targeting the role of neoatherosclerosis in late stent failure

Tobias Lenz[1], Philipp Nicol[1,2], Maria Isabel Castellanos[1,2], Ayat Aboutaleb Abdellah Abdelgalil[1], Petra Hoppmann[3], Wolfgang Kempf[1], Tobias Koppara[3], Anna Lena Lahmann[1], Alena Rüscher[1], Horst Kessler[4], and Michael Joner[1,2]*

[1]*Deutsches Herzzentrum München (German Heart Centre Munich), Klinik für Herz- und Kreislauferkrankungen, Technische Universität München, Lazarettstrae 36, 80363 Munich, Germany;*
[2]*DZHK (German Centre for Cardiovascular Research), Partner Site Munich Heart Alliance, Biedersteiner Strae 29, 80802 Munich, Germany;*
[3]*Klinik und Poliklinik für Innere Medizin I, Klinikum rechts der Isar, Technische Universität München, Ismaninger Str. 22, 81675 Munich, Germany; and*
[4]*Department of Chemistry and Center for Integrated Protein Science, Institute for Advanced Study, Technische Universität München, Lichtenbergstr. 4, 85747 Garching, Germany*

KEYWORDS
Coronary artery disease;
Neoatherosclerosis;
Late stent failure;
Intravascular imaging;
Magmaris BRS

Neoatherosclerosis is defined as foamy macrophage infiltration into the peri-strut or neointimal area after stent implantation, potentially leading to late stent failure through progressive atherosclerotic changes including calcification, fibroatheroma, thin-cap fibroatheroma, and rupture with stent thrombosis (ST) in advanced stages. Human autopsy as well as intravascular imaging studies have led to the understanding of neoatherosclerosis formation as a similar but significantly accelerated pathophysiology as compared to native atherosclerosis. This acceleration is mainly based on disrupted endothelial integrity with insufficient barrier function and augmented transmigration of lipids following vascular injury after coronary intervention and especially after implantation of drug-eluting stents. In this review, we summarize translational insights into disease pathophysiology and discuss therapeutic approaches to tackle this novel disease entity. We introduce a novel animal model of neoatherosclerosis alongside accompanying *in vitro* experiments, which show impaired endothelial integrity causing increased permeability for low-density lipoprotein cholesterol resulting in foam cell transformation of human monocytes. In addition, we discuss novel intravascular imaging surrogates to improve reliable diagnosis of early stage neoatherosclerosis. Finally, a therapeutic approach to prevent in-stent neoatherosclerosis with magnesium-based bioresorbable scaffolds and systemic statin treatment demonstrated the potential to improve arterial healing and re-endothelialization, leading to significantly mitigated neoatherosclerosis formation in an animal model of neoatherosclerosis.

*Corresponding author. Tel: +49 89 12180, Fax: +49 (0) 89/1218-4083, Email: joner@dhm.mhn.de

PALABRAS CLAVE
neoateroesclerosis;
fracaso tardío del stent;
técnicas de imagen intravascular;
BRS de Magmaris

La neoateroesclerosis se define como infiltración de macrófagos espumosos en la zona periprotésica o de la neoíntima tras una implantación de stent, lo cual posiblemente derive en un fracaso tardío del stent mediante cambios ateroescleróticos progresivos, incluidos la calcificación, fibroateromas, fibroateromas de cápsula fina (FACF) y trombosis del stent (TS). Gracias a los estudios de autopsia humana y de imagen intravascular se ha podido comprender la formación de la neoateroesclerosis de una manera fisiopatológica similar a la ateroesclerosis nativa pero significativamente acelerada. Esta aceleración se basa principalmente en la alteración de la integridad endotelial con una función de barrera insuficiente y una mayor transmigración de lípidos a consecuencia de una lesión vascular tras una intervención coronaria y, especialmente, tras la implantación de stents farmacoactivos. En este artículo ofrecemos un resumen de las perspectivas translacionales sobre la fisiopatología de la enfermedad y analizamos los enfoques terapéuticos para abordar esta nueva enfermedad. Presentamos un modelo animal de neoateroesclerosis innovador junto con experimentos *in vitro* complementarios, en los cuales se pone de manifiesto que la integridad endotelial dañada causa una mayor permeabilidad para el colesterol de las LDL (LDL), lo que da lugar a que los monocitos se transformen en células espumosas. Asimismo, comentamos los criterios indirectos de valoración de imagen intravascular a fin de mejorar el diagnóstico fiable de la neoateroesclerosis en fase inicial. Por último, en un enfoque terapéutico para prevenir la neoateroesclerosis del stent con andamios de magnesio biorreabsorbibles (BRS) y un tratamiento sistémico con estatinas se demostró la posibilidad de mejorar la cicatrización y la reendotelización arteriales, lo que derivó en la formación de neoateroesclerosis significativamente más lenta en un modelo animal de neoateroesclerosis.

关键词
冠状动脉疾病；
新动脉粥样硬化；
晚期支架衰竭；
血管内成像；
Magmaris 镁支架

新动脉粥样硬化被定义为支架植入后泡沫巨噬细胞浸润到支柱周围或新内膜区域，可能引起进行性动脉粥样硬化改变（包括钙化、纤维状动脉瘤、薄型纤维状动脉粥样硬化（TCFA））和晚期阶段的支架血栓破裂（ST）破裂而导致晚期支架衰竭。人体解剖以及血管内影像学研究使人们对新动脉粥样硬化的形成更为了解，新动脉粥样硬化的形成与自然动脉粥样硬化相似，但病理生理过程显著加快。这种加快主要是由于在冠状动脉介入治疗后，尤其是在植入药物洗脱支架后，发生血管损伤，内皮功能完整性受损，伴屏障功能不足及脂质转运增加。在这篇综述中，我们总结了对疾病病理生理学的转化见解，并讨论了解决这种新型疾病的治疗方法。我们引入了新的动脉粥样硬化动物模型并伴随了体外实验，该实验显示内皮完整性受损导致 LDL-胆固醇（LDL）的通透性增加，从而导致人单核细胞发生泡沫细胞转化。此外，我们讨论了新颖的血管内影像替代物，以期改善早期新动脉粥样硬化的可靠诊断。最后，使用可吸收镁支架（BRS）和全身他汀类药物治疗以预防支架内新动脉粥样硬化的治疗方法证明了改善动脉愈合和血管内皮化的潜力，从而使新动脉粥样硬化动物模型中新动脉粥样硬化的形成明显减轻。

Introduction

Drug-eluting stents—advances and setbacks

Milestones such as the development of drug-eluting stents (DES) and the refinement of antithrombotic therapy, as well as growing experience of interventional cardiologists have paved the way for the broad application of percutaneous coronary intervention (PCI) in treating coronary artery disease. While the introduction of antiproliferative agents with first-generation DES had led to a major decline in in-stent restenosis (ISR) due to suppression of neointimal overgrowth, a subsequent increase of late thrombotic complications as compared to bare metal stents (BMS) was observed.[1,2] This observation prompted research regarding its underlying pathophysiology.

Early human autopsy studies investigating first-generation DES, identified delayed arterial healing as an important limitation to these devices, revealing incomplete endothelialization and persistent fibrin deposition after implantation of first—and, to a somewhat lesser extent, second-generation DES. Furthermore, poor endothelialization, alongside other procedural and histological factors, seemed to correlate with an increased risk for the occurrence of late stent thrombosis (LST).[3,4] Subsequent in-depth histopathological analyses in animal models confirmed these observations. Bare metal stents showed better endothelial coverage than second—and especially first-generation DES. Areas around uncovered stent struts showed aggregation of platelets, fibrin, and inflammatory cells. Besides insufficient endothelial coverage, immunostaining, and organoid culture additionally indicated impaired endothelial integrity and decreased maturation following DES implantation irrespective of the examined stent generation.[5]

The first *in vivo* studies regarding this issue assessed arterial healing after stent implantation by coronary angioscopy. These studies likewise confirmed poor neointimal coverage after DES implantation. Furthermore, angioscopically assessed neointima 10 months after implantation of first-generation sirolimus-eluting stents showed accelerated as well as *de novo* yellow plaque formation within the nascent neointima, even in areas with visually complete endothelialization. Both the formation of yellow plaque and poor neointimal coverage independently translated into an increased risk of stent thrombosis.[6] It can thus be concluded that exposure of uncovered stent struts due to insufficient and dysfunctional endothelial coverage seems to accelerate new atherosclerotic changes within the neointima. In addition to the thrombogenic stimulus by uncovered struts themselves, these new atherosclerotic changes further increase the risk for adverse thrombotic events after DES implantation.[7]

Neoatherosclerosis—definition and clinical perspective

The observation of new atherosclerotic change within nascent neointimal tissue after stent implantation coined the term neoatherosclerosis. Histologically, neoatherosclerosis is defined as foamy macrophage infiltration into the peristrut or neointimal area, with or without calcification, fibroatheroma, thin-cap fibroatheroma (TCFA), and rupture with thrombosis in advanced stages.[8] Following further advancements in DES technology, target lesion revascularization rates both due to restenosis and stent thrombosis declined.[9] Nevertheless, autopsy studies continued to show higher rates of neoatherosclerosis in first- and second-generation DES compared to BMS and, more importantly, a continuous increase in cumulative incidence over time. The same studies also indicated that neoatherosclerosis not only increased the risk of late thrombotic events but seemed to contribute to the development of ISR, thus culminating in the pathophysiological continuum of late stent failure.[10–13] Large meta-analyses of clinical trials showed an overall risk of stent thrombosis in new-generation DES at 1 year of less than 1% and approximately 1% at 3 years.[2,9] In contrast, more than 90% of the patients presenting with stent thrombosis suffered myocardial infarction, making it a highly relevant clinical concern. In line with autopsy studies, clinical registries assessing the underlying pathology in patients presenting with stent thrombosis through optical coherence tomography (OCT) consistently found neoatherosclerosis causative of approximately 30% of late and very late stent thrombosis (VLST) cases. Interestingly, a high incidence of VLST was reported in BMS with substantially longer time since implantation compared to DES, placing implant duration on the top of the list of risk factors for neoatherosclerosis.[14–16]

Objectives

In light of the combined clinical and preclinical data, the higher incidence of neoatherosclerosis in autopsy studies following DES- compared to BMS implantation seems to be driven by a significantly accelerated development due to the combined mechanisms outlined above. Although previous studies provide important groundwork, substantial scientific gaps regarding late stent failure and neoatherosclerosis prevail and continued research is needed to understand its pathophysiology in sufficient detail. For this purpose, our research group aimed to refine established concepts of neoatherosclerosis pathophysiology, to gain further insight by combining preclinical *in vivo* as well as *in vitro* models with histology, immunohistochemistry, and latest intravascular imaging techniques. In a second step, we aimed to translate our findings into better imaging and differential diagnosis of late stent failure, improved device technology and prevention.

Our work

Basic principles

Human autopsy and animal studies shaped the understanding of neoatherosclerosis development as a multifactorial process.[12] Vascular injury after stent implantation cause endothelial denudation and migration of inflammatory cells. In case of DES, this process seems to be further augmented by chronic inflammation arising from biostable polymer coatings[17] and delayed arterial healing secondary to antiproliferative drug coatings, enabling increased infiltration of lipoproteins and migration of inflammatory cells through an impaired endothelial monolayer.[4,5] In addition, both BMS- and DES implantation cause blood flow disturbances and changes in sheer stress, possibly contributing to the migration of monocytes into the neointimal tissue as well.[18,19] The potential consequences are accumulation of lipid-laden macrophages within neointimal tissue, formation of fibroatheroma, and increased risk of myocardial infarction due to plaque rupture or erosion (*Figure 1*).

Since observations at autopsy are an important cornerstone of research dedicated to neoatherosclerosis, we evaluated a large autopsy stent registry at CVPath Institute (Gaithersburg, USA), with focus on prevalence and morphological characteristics of in-stent neoatherosclerosis. Separating cases of fibroatheroma, in-stent plaque rupture and TCFA, we observed that the majority of necrotic cores are located superficially inside the neointimal tissue and that neoatherosclerotic plaques are only infrequently in continuation of atherosclerotic plaque within the native coronary artery. This emphasizes the clinical importance of this disease entity and indicates a post-interventional development, following mechanisms at least partly independent from those of the underlying primary atherosclerotic disease.[12] Comparing the different stent types, we observed no significant differences in neoatherosclerosis prevalence between new- and early generation DES. Regarding the time course of neoatherosclerosis development, previous studies revealed a significantly earlier manifestation following DES- as compared to BMS implantation. First signs of neoatherosclerosis in BMS occurred as late as 900 days after implantation, compared to 70–120 days in early generation DES.[8] First data from autopsy studies including second-generation DES showed no significant differences in neoatherosclerosis frequency between different DES types.[10] The analysis of a total of 384 autopsy

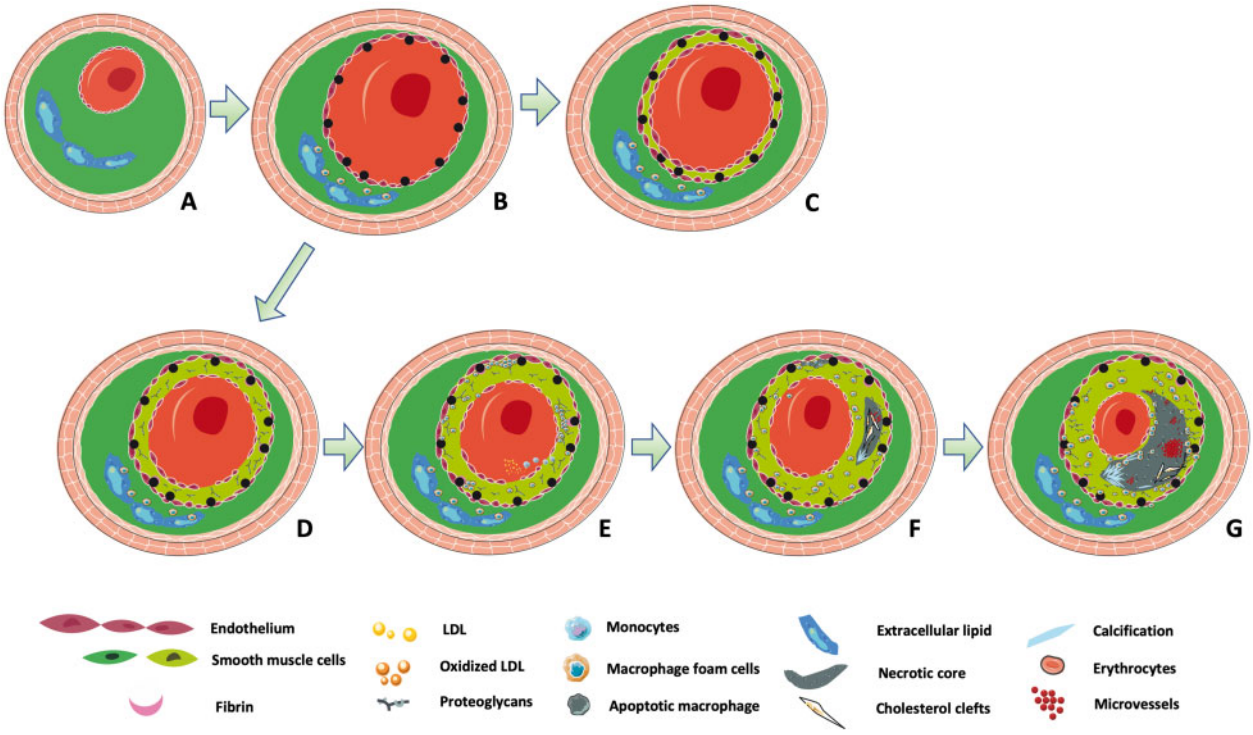

Figure 1 Pathophysiological pathway of in-stent neoatherosclerosis. (*A*) Atherosclerotic artery with lumen narrowing. (*B*) Artery directly after successful stent implantation without re-endothelialization and/or neointima. (*C*) Complete arterial healing with a thin layer of mature neointima and sufficient re-endothelialization. (*D*) Less than 3 months after stenting, leaky re-endothelialization, immature, proteoglycan-rich neointima, and fibrin deposition around some stent struts. (*E*) Three to 4 months after stenting, macrophage and LDL cholesterol migration through disrupted endothelium, causing accumulation of lipid-laden foamy macrophages predominantly close to the intraluminal surface and in the peri-strut regions. (*F*) Nine to 12 months after stenting, necrotic core following apoptosis of foamy macrophages, beginning neovascularization, and calcification. (*G*) More than 1 year after stenting, in-stent thin-cap fibroatheroma with calcification, neovascularization, haemorrhage, and ongoing surrounding inflammation.

cases comprised of 614 stented lesions in native coronary arteries confirmed these results. We observed a comparable prevalence of neoatherosclerosis in first and second-generation DES up to 3 years implant duration. Within the indicated time-span, neoatherosclerosis was observed with a significantly lower frequency in BMS than either type of DES. Between 1 and 3 years after implantation, neoatherosclerosis was observed with similar prevalence of 51% in first- and 48% in second-generation DES compared to only 6% in BMS. For duration of implant >3 years, prevalence of neoatherosclerosis was still lower in BMS than in first-generation DES (65%) but rose as high as 48%, while there was absence of samples of second-generation DES with implant duration >3 years.[11,12] This is in line with the mitigation of the difference in neoatherosclerosis prevalence between BMS and DES over time, observed in intravascular imaging studies.[14-16] The basic pathological mechanisms of neoatherosclerosis development are likely to be similar for different types of metallic DES, explaining the absence of significant differences between first- and second-generation DES in autopsy studies. On the other hand, comparisons of different DES show differing vascular responses to implantation, including various potentially contributing factors to neoatherosclerosis pathogenesis. Autopsy and animal studies show varying rates and patterns of re-endothelialization, inflammation, hypersensitivity reaction, and fibrin deposition.[5,10,20,21] Further research is warranted to sort the individual impact of different stent components on neoatherosclerosis formation.

The two most prominent causes of late stent failure are ISR and VLST, which both seemed to be associated with neoatherosclerosis in our registry. Overall 10 out of 614 lesions showed VLST (>1 year) caused by in-stent neoatherosclerosis (1.6%) with similar incidence in BMS (1.8%) and first-generation DES (1.9%), albeit a different mean implant duration of 832 days for BMS and 383 days for first-generation DES. In relation to the total number of VLST, in-stent plaque rupture was identified as the underlying cause in 83% of VLST in BMS and in 15% of VLST in first-generation DES. Beyond 3 years, 100% of VLST in BMS and 33% of VLST in first-generation DES were caused by neoatherosclerotic in-stent plaque rupture. For second-generation DES, we observed no VLST while mean implant duration only reached up to 210 days[12] (*Figure 2*).

In-stent restenosis within the first year after implantation was observed with a prevalence of 46.9% in BMS, 16.2% in first-generation DES, and 19.1% in second-generation DES. Simultaneous occurrence of neoatherosclerosis and ISR was more frequent in BMS (6.8%) than in first- and second-generation DES (4.2% and 3.2%) with an overall prevalence of 5.2% and the known significant differences in implant duration among stent types. Restenosis with

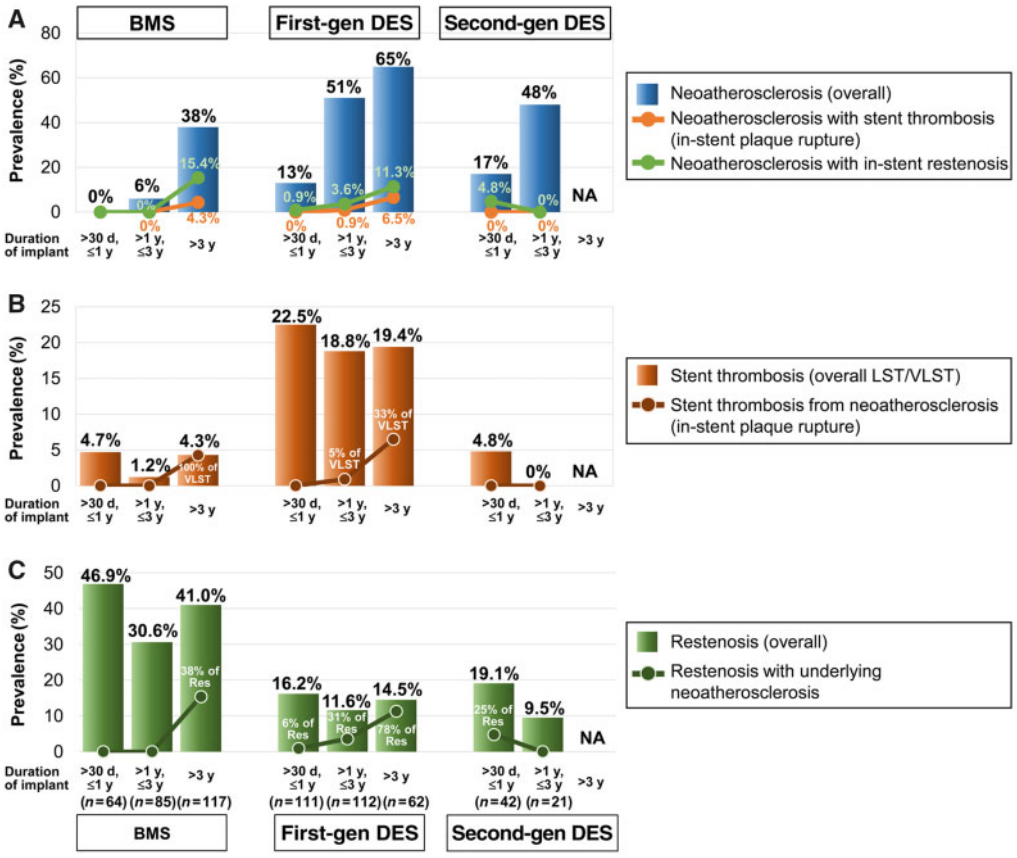

Figure 2 (*A*) Prevalence of neoatherosclerosis in bare metal stent, first- and second-generation drug-eluting stents stratified by duration of implant (bar graphs) along with the prevalence of restenosis (green line) and thrombosis (orange line) in the lesions with neoatherosclerosis and late stent failure. (*B*) Prevalence of overall stent thrombosis, in association with neoatherosclerosis (in-stent plaque rupture). (*C*) Prevalence of in-stent restenosis and its association with underlying neoatherosclerosis. LST/VLST, late and very late stent thrombosis; Res, restenosis. Reproduced with permission from Otsuka *et al*.[12]

neoatherosclerosis in BMS was only observed 3 years or beyond, representing 38% of late restenosis cases in BMS. In comparison, restenosis in combination with neoatherosclerosis in first-generation DES was observed already within in the first year, similarly increasing over time and resulting in 78% of first-generation DES restenosis cases simultaneously showing neoatherosclerosis. Due to small overall numbers, no very late restenosis was observed in second-generation DES[12] (*Figure 2*).

Both ISR and VLST demonstrate a time-dependent association with neoatherosclerosis in BMS as well as in DES, with an earlier and more frequent simultaneous manifestation in the latter. This strongly indicates a pathophysiological contribution of in-stent neoatherosclerosis to late stent failure.[11,12]

Endothelial integrity

In order to understand neoatherosclerosis pathophysiology in greater detail, we continued to separately investigate the different mechanisms postulated on the basis of previous research. In cell culture experiments and specific animal models of neoatherosclerosis, we assessed the impact of endothelial integrity on neoatherosclerosis formation. Previous preclinical studies showed a promising improvement of endothelialization after implantation of cRGD-coated as compared to BSA-coated stents.[22] RGD is a tripeptide (arginine–glysine–aspartate) known to mediate binding of endothelial integrins to various components of the extracellular matrix. Building on this knowledge, we sought to investigate whether RGD-coated stents could improve endothelial integrity with specific focus on its barrier function against hypercholesterolaemia. Therefore, a novel animal model of neoatherosclerosis was established, in which New Zealand White Rabbits underwent a sequence of hypercholesteraemic diet and arterial denudation to cause formation of neointimal foam cells. In this setting, commercially available everolimus-eluting stents (EES) (Xience Prime, 3.0 × 15 mm, Abbott Vascular, CA, USA) and customized RGD-coated stents were randomly allocated to rabbits iliac arteries.

Histopathological assessment of the different stent types showed a significantly greater expression of CD31 (PECAM-1) after implantation of RGD-coated stents as compared to EES, suggesting a greater overall endothelial coverage. This was confirmed by scanning electron microscopy (SEM) revealing a higher percentage of covered RGD-coated stent struts as opposed to EES. Furthermore, co-registration of confocal microscopy and SEM as well as Z-stack tile imaging revealed a predominance of FITC-dextran, an established marker of membrane permeability, in areas without

CD31-positive endothelial cells. More importantly, the majority of FITC-dextran appeared clearly located underneath the endothelial monolayer in EES as opposed to RGD-coated stents, where the FITC-dextran signal was observed almost superimposing the endothelial cells. This indicates improved endothelial integrity after implantation of RGD-coated stents, in contrast to a significant delay in arterial healing, exemplified by incomplete endothelial coverage and increased permeability after implantation of commercially available EES.

To further break down the constituent mechanisms causing this observation, adjunct *in vitro* experiments were conducted. Human umbilical vein endothelial cells (HUVECs) and human coronary artery cells (HCAECs) were cultured onto semipermeable membranes, coated with linear peptide RGD or a non-specific peptide sequence as a negative control and placed in between two medium-filled chambers. The endothelial cells were treated with different concentrations of everolimus to simulate the effect of DES-coating on the endothelial cell monolayer.

Microscopy and immunofluorescence revealed dose-dependent structural modification and impairment of the actin cytoskeleton and adhesive cell-to-cell junctions by everolimus, exemplified by vascular endothelial cadherin expression, with obvious gaps in the endothelial monolayer for highest concentrations. Spectrometric measurement of diffusion of fluorescently labelled low-density lipoprotein (AcLDL) from the upper to the bottom chamber showed an increased LDL permeability through everolimus treatment. Endothelial cells grown on RGD-coated membranes demonstrated a more consistent confluence and a decreased permeability for LDL. Consistent with animal data, the *in vitro* permeability assays thus support the perception of a dose-dependent impairment of endothelial integrity caused by everolimus as well as a mitigation of this effect by RGD-coating.

One step further down the pathway of neoatherosclerosis pathogenesis, we assessed the effect of increasing concentrations of everolimus in combination with a fixed concentration of AcLDL on monocytes placed into the lower of two chambers, separated by HUVECs and HCAECs seeded onto semipermeable membranes. Owing to the increased permeability of the endothelial monolayer for LDL, caused by everolimus, we observed a dose-dependent transformation of monocytes into foam cells. Again, this effect was attenuated through RGD-coating of the semipermeable membranes (manuscript submitted).

From bench to bedside

An important link between histopathology and clinical practice, regarding diagnosis of neoatherosclerosis is intravascular imaging. Optical coherence tomography is able to depict macrophage infiltration and lipid-laden tissue within the neointima and is therefore considered the current diagnostic gold standard, even though numerous limitations to *in vivo* assessment of neoatherosclerosis still apply.

An imperative for further understanding of neoatherosclerosis pathophysiology are diagnostic tools for its *in vivo* assessment in humans. In addition, the same tools offer great potential to monitor efficacy control of device as well as other therapeutic innovations. For this reason, another key part of our research effort is focused on intravascular imaging.

The PRESTIGE consortium is a multicentre, interdisciplinary global European effort for the prevention of LST. In order to improve understanding of mechanistic processes leading to stent thrombosis, OCT imaging was performed in patients presenting with ST, following a prospective study protocol. In cases of VLST (ST $>$ 1 year), neoatherosclerosis was adjudicated the dominant finding in 31.3% of cases, thus being the most common denominator underlying VLST in this particular group of patients.[14]

To further investigate aetiological factors of neoatherosclerosis and its contribution to (very) late stent failure, our group carried out an analysis of the PRESTIGE data, limited to this prespecified subgroup. Optical coherence tomography findings showed neoatherosclerosis in 43.4% of patients presenting with VLST. In 68% of those patients and 30% of all patients, rupture of neoatherosclerotic plaque was identified as the underlying cause of VLST. Although neoatherosclerosis was observed more frequently in BMS than in DES, most likely due to an almost twice as long duration from index stenting to VSLT (4.52 years vs. 8.24 years; $P < 0.0001$) in BMS relative to DES, multivariate Cox regression analysis revealed a 2.2-fold increased risk to develop neoatherosclerosis after implantation of DES. Multivariate regression analysis of predictors for plaque rupture revealed a 4.9-fold higher risk for patients combining neoatherosclerosis and previous myocardial infarction. Univariate analysis showed a significant infiltration of macrophages in OCT-frames showing in-stent plaque rupture ($P < 0.0001$). These findings emphasize the detrimental impact of neoatherosclerosis on future disease progression. Secondly, the increased risk for neoatherosclerosis after DES implantation in our study is in line with autopsy studies and seems to support the established models of neoatherosclerosis pathophysiology outlined above. Macrophage infiltration could serve as an imaging surrogate for plaque instability and intensified secondary prevention after observation of neoatherosclerosis in patients with history of myocardial infarction, e.g. during follow-up angiography could lead to improved outcomes in this group of high-risk patients.[23]

Establishing intravascular imaging surrogates

The most important limitation to intravascular imaging for the detection of neoatherosclerosis, as well as other histological patterns, is the lack of well-established surrogate parameters. The only valid methods to acquire these parameters start from careful co-registration of histology and intravascular imaging. Thereafter, distinctive histological features have to be identified and correlated with corresponding imaging characteristics. In addition, in order to provide reproducibility and observer independence, any automated approach should be given preference over subjective visual assessment. The current method of choice for the detection of neoatherosclerosis is OCT. Owing to its superior spatial resolution, OCT enables

detection of early signs of neoatherosclerosis formation such as macrophage infiltration. In addition, it allows detailed morphological assessment of features related to neoatherosclerosis such as calcification and neovascularization. Furthermore, it permits distinction of vulnerable atherosclerotic plaque types as identified by fibrous cap thickness. Due to its tissue penetration depth up to 5 mm, intravascular ultrasound can be useful to detect late-stage neoatherosclerosis and to quantify neoatherosclerotic plaque but lacks the appropriate resolution to visualize the above-mentioned features.[24]

To assess the first level of neoatherosclerosis development—arterial healing—a previous study of our group correlated histology and OCT of atherosclerotic rabbit arteries at different timepoints after implantation of DES and BMS as well as autopsy specimen. In case of autopsy specimens, OCT was acquired post-mortem. To distinguish mature from immature neointima, we attempted to characterize smooth muscle cell-rich, mature neointima by grey scale intensity (GSI) measurement of corresponding intravascular OCT images. This proof-of-concept study was the first to show that OCT-derived GSI analysis can distinguish mature from immature neointimal tissue with high sensitivity and specificity.[25]

An early and established sign of neoatherosclerosis manifestation is infiltration of nascent neointimal tissue with foamy macrophages. While detection of neointimal maturity acts at a very early stage, reliable *in vivo* assessment of neointimal foamy macrophages provides the potential of early identification of patients at risk for late stent failure. Previous research has shown that macrophage infiltration in native coronary arteries can be visualized by automatic quantification of the OCT signal attenuation.[26,27] In a recent human autopsy study, we assessed the question whether OCT signal attenuation can also be used to detect neointimal foamy macrophages. Our analysis revealed that histologically identified regions with and without lipid-laden macrophages had significantly different tissue attenuation indices and could therefore serve to detect early stages of neoatherosclerosis *in vivo*. These findings are so far limited to a selected set of patients, as high sensitivity and specificity could only be achieved in cases of overall homogenous neointima. In case of other OCT patterns, grouped together as non-homogenous, reasonable specificity at least indicates the value of this methodology for the exclusion of neointimal foamy macrophages. Measurement of tissue attenuation index in clinical cases of patients presenting with ISR, using the cut-off values derived from histological co-registration, showed a realistic proportion of neointimal foam cell infiltration in homogenous neointima. These results suggest applicability of this objective and automated approach as a supportive tool to identify neoatherosclerosis formation in selected patients (manuscript submitted).

Systemic vs. site-targeted treatment of neoatherosclerosis

Drug-eluting stents have been an important and indispensable improvement compared to its predecessor technology, the BMS, but seem to be a major contributor to the development of neoatherosclerosis. The ideal coronary stent would provide sufficient radial strength to resist vessel recoil and effectively prevent intimal hyperplasia, without causing long-term inflammation, endothelial dysfunction, and vessel caging. Since a large part of these contemporary DES-shortcomings are attributed to its permanent presence in the vascular wall, bioresorbable drug-eluting scaffolds (BRS) appear to be the next logical step and an attractive approach for the prevention of in-stent neoatherosclerosis.

Mainly two different approaches have been followed to develop bioresorbable scaffolds: polymeric vs metallic. The most commonly used materials in currently available bioresorbable coronary stent scaffolds are poly-L-lactic-acid (PLLA) and magnesium, associated with important differences in radial as well as tensile strength, elasticity and degradation kinetics.[28] The BRS with the largest available clinical evidence so far is the everolimus-eluting Absorb bioresorbable vascular scaffold (BVS) (Abbott Vascular, Santa Clara, CA, USA), made of a PLLA-polymer. After initial results were highly promising, major randomized trials and meta-analyses revealed significantly increased rates of target lesion failure and scaffold thrombosis (ScT) as compared to metallic biostable EES,[29–31] which lead to current guidelines on myocardial revascularization restricting the use of any bioresorbable scaffolds to well-controlled clinical studies.[32] The underlying mechanisms are multifactorial. An important lesson of the first years of experience with Absorb BVS was, that ScT could be reduced through a BVS-specific implantation technique.[33] Furthermore, intravascular imaging studies revealed strut discontinuities, malaposition, as well as neoatherosclerosis as the most frequent underlying pathologies of late Absorb BVS thrombosis. While interaction between implantation technique and LSF through malaposition and strut discontinuities seems plausible, it is unlikely for neoatherosclerosis.[34]

From a mechanical point of view, magnesium and corresponding alloys used for the manufacturing of metallic BRS offer better radial and tensile strength combined with better elongation at break compared to PLLA.[35] The magnesium scaffold with the most available preclinical and clinical data, and the first to receive CE-mark approval, is the Magmaris BRS (Biotronik, Bülach, Swizerland). The Magmaris BRS is a magnesium-alloy-based scaffold with a six-crown two-link design, square-shaped struts with 150 μm thickness and a degradable PLLA-coating with a sirolimus-concentration of 1.4 $\mu g/mm^2$. Preclinical evaluation of this new-generation magnesium scaffold suggests a reasonable safety profile and improved vascular compatibility owed to advanced healing, mitigated thrombogenicity and inflammatory response as well as favourable degradation kinetics.[36–40] In addition to some degree of assumed inherent antithrombogenic and anti-inflammatory properties of the magnesium backbone itself, improved degradation kinetics are considered a key feature. While the Absorb BVS has a degradation time-span of as much as 3 years,[41] Magmaris showed 95% complete degradation to amorphous calcium phosphate at one year after implantation in healthy porcine coronary arteries.[39] Whether these preclinical findings translate into improved clinical outcome is currently being assessed in dedicated trials, so far

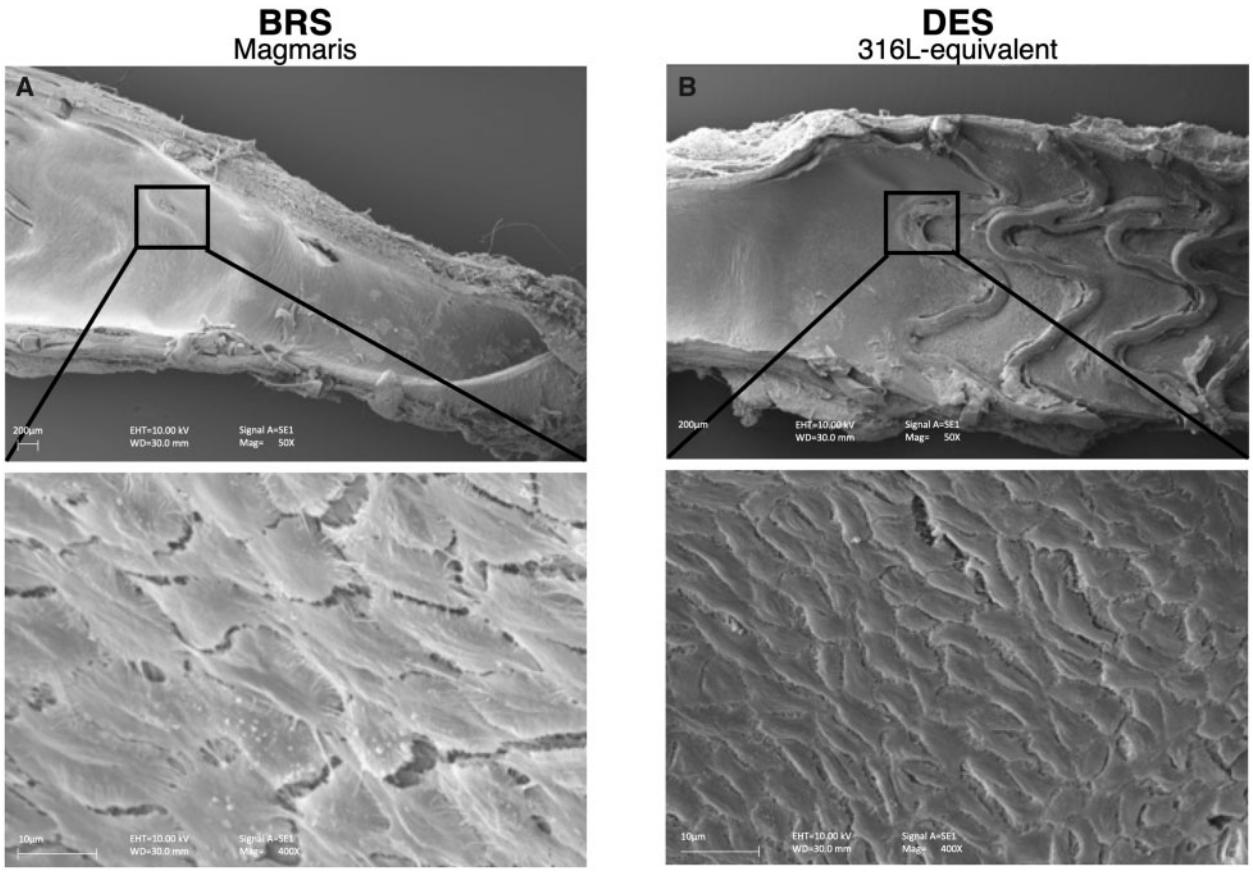

Figure 3 Representative scanning electron microscopy images of after implantation of Magmaris bioresorbable drug-eluting scaffolds (*A*) and custom-design stainless steel drug-eluting stent (*B*).

showing promising results as outcomes seem to be at least comparable to those of the current standard-of-care DES.[42–45] However, randomized controlled trials with sufficient power to prove these observations are still lacking and in parallel, a new generation of polymer-based bioresorbable scaffolds with thinner struts as well as improved radial strength and degradation kinetics are being developed.[28]

Nevertheless, the favourable fast resorption of magnesium-based bioresorbable scaffolds and thereby relatively early restoration of physiological vascular function after magnesium-based scaffold implantation, appears to offer significant potential for the prevention of in-stent neoatherosclerosis. To test this hypothesis, we compared the Magmaris fully bioresorbable magnesium scaffold to a custom-designed stainless-steel stent of equivalent geometry, both sirolimus-eluting, in an animal model of neoatherosclerosis. The applied model of neoatherosclerotic rabbits was similar to the one previously established, in which a high cholesterol diet and serial arterial denudation after implantation of the study device, simulate the events that lead to neoatherosclerosis formation after PCI in humans. In order to isolate the impact of the Magmaris bioresorbable magnesium backbone on this process, we chose a comparator stent of equal geometry and design as well as drug-eluting polymer coating. We hypothesized that the improved biocompatibility of Magmaris BRS, suggested by previous preclinical research involving healthy animals, would be transferable to a model of diseased neoatherosclerotic arteries and lead to improved re-endothelialization as well as minimized thrombus formation and inflammation after inevitable arterial injury caused by stent implantation. Both the contribution of LDL cholesterol to the pathogenesis of atherosclerosis and development of coronary heart disease and the beneficial effect of LDL-lowering through statin-therapy are well-established. In order to compare device-based effects of this site-targeted approach with established systemic therapy, animals were sequentially randomized to systemic statin treatment and placebo after completion of serial denudation. In addition, we aimed to investigate synergistic effects of a supplementary statin therapy on neoatherosclerosis progression.

As per histological analysis as well as OCT immediately following euthanasia, bioresorbable magnesium scaffolds indeed showed a significant decrease of neointimal foamy macrophage infiltration compared to DES. Alongside mitigated neoatherosclerosis formation, we also observed greater endothelial integrity in BRS than in equivalent DES, through SEM (*Figure 3*). In addition, rabbits that received high-dose atorvastatin showed reduced neoatherosclerosis formation in both DES and BRS. Reduction of neointimal foamy macrophage infiltration in BRS compared to DES was greater and independent of reduction through statin-therapy vs. placebo. Significant statistical interaction between stent type and medical treatment allocation

suggests a synergistic effect of site-targeted device and systemic statin therapy. However, it is of note that the reduction of neointimal macrophage infiltration and quicker endothelialization observed in our animal model, appeared to be achieved at the collateral cost of a greater neointimal area in BRS relative to DES, resulting in increased percentage stenosis.

In a similar animal model, we aimed to take a closer look at the differences in re-endothelialization after DES- vs. BRS implantation. Consistent with previous results, electron microscopy showed an overall greater endothelial coverage in BRS. Additional immunofluorescent visualization of CD31 (PECAM-1) revealed numerically greater expression above BRS-struts, suggesting improved maturity and integrity. Furthermore, permeability for FITC-dextran assessed by confocal microscopy seemed to be promoted in CD31-negative areas. This supports the suitability of CD31 as a marker of endothelial integrity as permeability for FITC-dextran is a well-established marker for an impaired barrier function (manuscript submitted).

Outlook

In support of and in addition to animal and human autopsy studies, *in vitro* experiments such as permeability assays help to depict pathological pathways in greater detail. Further detail could be provided by cytokine assays, examining the expression of different pro- and anti-inflammatory proteins by endothelial cells or monocytes, i.e. in correlation to different concentrations of antiproliferative drugs.

Alterations in flow dynamics, causing promoted adhesion of inflammatory cells and delayed re-endothelialization in areas of blood flow disturbances or low flow rates due to stent struts, very likely impact arterial healing and neoatherosclerosis development.[18,19] Focus on this field will lead to further improvement of device biocompatibility. Especially new-generation biodegradable scaffolds, which remain an appealing concept in spite of so far ambiguous clinical outcome, leave considerable room for optimization in this regard.

Furthermore, great focus will lay on continued enhancement of coronary stent device technology. Biostable new-generation DES are constantly being improved with a trend towards ever thinner stent struts and better biocompatibility of polymer coating.[46] In parallel, solutions for shortcomings of current bioresorbable scaffolds such as the lower limits of strut thickness to achieve sufficient radial support are being developed.[28] Moreover, recent device innovations followed a pro-healing approach. The first device of that kind to achieve CE-mark approval is the COMBO dual therapy stent (OrbusNeich, Hong Kong, China). This device aims at the suppression of neointimal overgrowth through an abluminal layer of sirolimus eluted from a biodegradable polymer, while a luminal coating with immobilized anti-CD34+ antibodies serves as anchor for circulating endothelial progenitor cells. So far none of those promising innovations have surpassed current gold-standard DES, but results of ongoing dedicated clinical trials are eagerly awaited.[47]

Before making the effort to assess the effect of improvements in device technology and prevention on clinical outcome, preclinical evaluation on a molecular level without the need for histology would be of great value. A variety of multimodality molecular imaging techniques have found its way into cardiovascular medicine. In most cases, these techniques combine an established light- or ultrasound-based optical imaging modality with a second modality, able to provide information about the molecular tissue composition based on fluorescence or spectroscopy.[24,48,49] At the same pace, non-invasive functional imaging techniques are refined, so far limited to native coronary arteries, which add as well to the shaping of our pathophysiological understanding and development of therapeutic approaches.[50] Last but not least, algorithm-based automated detection of distinct histological patterns in intravascular coronary images using artificial intelligence techniques are yet to mature, but hold tremendous potential as a tool to improve validity of intravascular imaging as well as to identify patients at risk for future coronary events.

Conclusions and clinical implications

In summary, neoatherosclerosis can be considered an accelerated form of atherosclerosis due to incomplete endothelialization, disrupted endothelial integrity, as well as stent-induced inflammatory processes after PCI and especially after implantation of DES. In light of a persistently high worldwide incidence and prevalence of coronary heart disease, the role of neoatherosclerosis in late stent failure with potentially serious complications is a matter of significant clinical concern. The dilemma becomes particularly evident, reflecting that treatment of occlusive atherosclerotic coronary lesions itself, seems to induce in-stent neoatherosclerotic changes following similar but accelerated pathophysiological mechanisms. Persistent limitations to modern-generation coronary stents revealed by preclinical as well as clinical research call for continued translational research efforts, aiming at optimization of device-biocompatibility, to achieve the exact balance between suppression of neointimal overgrowth and sufficient re-endothelialization with functional neointima after coronary stent implantation. The reduction of early neoatherosclerotic changes through magnesium-based bioresorbable scaffolds observed in our animal model of neoatherosclerosis, supported by synergistic effects of systemic statin therapy, can be considered a promising step in that direction.

Funding

This paper was published as part of a supplement supported by an educational grant from Boehringer Ingelheim.

Conflict of interest: M.J. reports personal fees from Consulting for Biotronik, personal fees from Speakers fee from Biotronik, personal fees from Consulting for Orbus Neich, personal fees from

Speakers fee from Orbus Neich, an educational grant from Boston Scientific.

References

1. Cassese S, Byrne RA, Tada T, Pinieck S, Joner M, Ibrahim T, King LA, Fusaro M, Laugwitz KL, Kastrati A. Incidence and predictors of restenosis after coronary stenting in 10 004 patients with surveillance angiography. *Heart* 2014;**100**:153–159.
2. Tada T, Byrne RA, Simunovic I, King LA, Cassese S, Joner M, Fusaro M, Schneider S, Schulz S, Ibrahim T, Ott I, Massberg S, Laugwitz KL, Kastrati A. Risk of stent thrombosis among bare-metal stents, first-generation drug-eluting stents, and second-generation drug-eluting stents: results from a registry of 18,334 patients. *JACC Cardiovasc Interv* 2013;**6**:1267–1274.
3. Finn AV, Joner M, Nakazawa G, Kolodgie F, Newell J, John MC, Gold HK, Virmani R. Pathological correlates of late drug-eluting stent thrombosis: strut coverage as a marker of endothelialization. *Circulation* 2007;**115**:2435–2441.
4. Joner M, Finn AV, Farb A, Mont EK, Kolodgie FD, Ladich E, Kutys R, Skorija K, Gold HK, Virmani R. Pathology of drug-eluting stents in humans. Delayed healing and late thrombotic risk. *J Am Coll Cardiol* 2006;**48**:193–202.
5. Joner M, Nakazawa G, Finn AV, Quee SC, Coleman L, Acampado E, Wilson PS, Skorija K, Cheng Q, Xu X, Gold HK, Kolodgie FD, Virmani R. Endothelial cell recovery between comparator polymer-based drug-eluting stents. *J Am Coll Cardiol* 2008;**52**:333–342.
6. Higo T, Ueda Y, Oyabu J, Okada K, Nishio M, Hirata A, Kashiwase K, Ogasawara N, Hirotani S, Kodama K. Atherosclerotic and thrombogenic neointima formed over sirolimus drug-eluting stent. An angioscopic study. *JACC Cardiovasc Imaging* 2009;**2**:616–624.
7. Nakazawa G, Vorpahl M, Finn AV, Narula J, Virmani R. One step forward and two steps back with drug-eluting-stents. From preventing restenosis to causing late thrombosis and nouveau atherosclerosis. *JACC Cardiovasc Imaging* 2009;**2**:625–628.
8. Nakazawa G, Otsuka F, Nakano M, Vorpahl M, Yazdani SK, Ladich E, Kolodgie FD, Finn AV, Virmani R. The pathology of neoatherosclerosis in human coronary implants. *J Am Coll Cardiol* 2011;**57**:1314–1322.
9. Byrne RA, Serruys PW, Baumbach A, Escaned J, Fajadet J, James S, Joner M, Oktay S, Jüni P, Kastrati A, Sianos G, Stefanini GG, Wijns W, Windecker S. Report of a European Society of Cardiology-European Association of Percutaneous Cardiovascular Interventions task force on the evaluation of coronary stents in Europe: executive summary. *Eur Heart J* 2015;**36**:2608–2620.
10. Otsuka F, Vorpahl M, Nakano M, Foerst J, Newell JB, Sakakura K, Kutys R, Ladich E, Finn AV, Kolodgie FD, Virmani R. Pathology of second-generation everolimus-eluting stents versus first-generation sirolimus- and paclitaxel-eluting stents in humans. *Circulation* 2014;**129**:211–223.
11. Otsuka F, Sakakura K, Yahagi K, Sanchez OD, Kutys R, Ladich E, Fowler DR, Kolodgie FD, Davis HR, Joner M, Virmani R. Contribution of in-stent neoatherosclerosis to late stent failure following bare metal and 1st- and 2nd-generation drug-eluting stent placement: an autopsy study. *J Am Coll Cardiol* 2014;**64**:B190–B191.
12. Otsuka F, Byrne RA, Yahagi K, Mori H, Ladich E, Fowler DR, Kutys R, Xhepa E, Kastrati A, Virmani R, Joner M. Neoatherosclerosis: overview of histopathologic findings and implications for intravascular imaging assessment. *Eur Heart J* 2015;**36**:2147–2159.
13. Xhepa E, Byrne RA, Rivero F, Rroku A, Cuesta J, Ndrepepa G, Kufner S, Bastante T, Salvatore V, Marcos C, Guimaraes G, Lena A, Himanshu L, Heribert R, Joner M, José M, Vizcayno P, Gonzalo N, Alfonso F, Kastrati A. Qualitative and quantitative neointimal characterization by optical coherence tomography in patients presenting with in-stent restenosis. *Clin Res Cardiol* 2019;**108**:1059–1068.
14. Adriaenssens T, Joner M, Godschalk TC, Malik N, Alfonso F, Xhepa E, De Cock D, Komukai K, Tada T, Cuesta J, Sirbu V, Feldman LJ, Neumann FJ, Goodall AH, Heestermans T, Buysschaert I, Hlinomaz O, Belmans A, Desmet W, Ten Berg JM, Gershlick AH, Massberg S, Kastrati A, Guagliumi G, Byrne RA; Prevention of Late Stent Thrombosis by an Interdisciplinary Global European Effort (PRESTIGE) Investigators. Optical coherence tomography findings in patients with coronary stent thrombosis: a report of the PRESTIGE consortium (Prevention of Late Stent Thrombosis by an Interdisciplinary Global European effort). *Circulation* 2017;**136**:1007–1021.
15. Souteyrand G, Amabile N, Mangin L, Chabin X, Meneveau N, Cayla G, Vanzetto G, Barnay P, Trouillet C, Rioufol G, Rangé G, Teiger E, Delaunay R, Dubreuil O, Lhermusier T, Mulliez A, Levesque S, Belle L, Caussin C, Motreff P. Mechanisms of stent thrombosis analysed by optical coherence tomography: insights from the national PESTO French registry. *Eur Heart J* 2016;**37**:1208–1216a.
16. Taniwaki M, Radu MD, Zaugg S, Amabile N, Garcia-Garcia HM, Yamaji K, Jrgensen E, Kelbæk H, Pilgrim T, Caussin C, Zanchin T, Veugeois A, Abildgaard U, Jüni P, Cook S, Koskinas KC, Windecker S, Räber L. Mechanisms of very late drug-eluting stent thrombosis assessed by optical coherence tomography. *Circulation* 2016;**133**:650–660.
17. Nakazawa G, Ladich E, Finn AV, Virmani R. Pathophysiology of vascular healing and stent mediated arterial injury. *EuroIntervention* 2008;**4(Suppl C)**:C7–C10.
18. Jiménez JM, Davies PF. Hemodynamically driven stent strut design. *Ann Biomed Eng* 2009;**37**:1483–1494.
19. Davies PF. Hemodynamic shear stress and the endothelium in cardiovascular pathophysiology. *Nat Clin Pract Cardiovasc Med* 2009;**6**:16–26.
20. Nakazawa G, Finn AV, Vorpahl M, Ladich ER, Kolodgie FD, Virmani R. Coronary responses and differential mechanisms of late stent thrombosis attributed to first-generation sirolimus- and paclitaxel-eluting stents. *J Am Coll Cardiol* 2011;**57**:390–398.
21. Mori H, Atmakuri DR, Torii S, Braumann R, Smith S, Jinnouchi H, Gupta A, Harari E, Shkullaku M, Kutys R, Fowler D, Romero M, Virmani R, Finn AV. Very late pathological responses to cobalt-chromium everolimus-eluting, stainless steel sirolimus-eluting, and cobalt-chromium bare metal stents in humans. *J Am Heart Assoc* 2017;**6**:doi:10.1161/JAHA.117.007244.
22. Joner M, Cheng Q, Scho S, Lopez M, Neubauer S, Mas-Moruno C, Laufer B, Kolodgie FD, Kessler H, Virmani R. Polymer-free immobilization of a cyclic RGD peptide on a nitinol stent promotes integrin-dependent endothelial coverage of strut surfaces. *J Biomed Mater Res B Appl Biomater* 2012;**100**:637–645.
23. Joner M, Koppara T, Byrne RA, Castellanos MI, Lewerich J, Novotny J, Guagliumi G, Xhepa E, Adriaenssens T, Godschalk TC, Malik N, Alfonso F, Tada T, Neumann F-J, Desmet W, ten Berg JM, Gershlick AH, Feldman LJ, Massberg S, Kastrati A. Neoatherosclerosis in patients with coronary stent thrombosis: findings from optical coherence tomography imaging (a report of the PRESTIGE Consortium). *JACC Cardiovasc Interv* 2018;**11**:1340–1350.
24. Nicol P, Xhepa E, Bozhko D, Joner M. Neoatherosclerosis: from basic principles to intravascular imaging. *Minerva Cardioangiol* 2018;**66**:292–300.
25. Malle C, Tada T, Steigerwald K, Ughi GJ, Schuster T, Nakano M, Massberg S, Jehle J, Guagliumi G, Kastrati A, Virmani R, Byrne RA, Joner M. Tissue characterization after drug-eluting stent implantation using optical coherence tomography. *Arterioscler Thromb Vasc Biol* 2013;**33**:1376–1383.
26. Di Vito L, Agozzino M, Marco V, Ricciardi A, Concardi M, Romagnoli E, Gatto L, Calogero G, Tavazzi L, Arbustini E, Prati F. Identification and quantification ofmacrophage presence in coronary atherosclerotic plaques by optical coherence tomography. *Eur Heart J Cardiovasc Imaging* 2015;**16**:807–813.
27. van Soest G, Goderie T, Regar E, Koljenović S, van Leenders G, Gonzalo N, van Noorden S, Okamura T, Bouma BE, Tearney GJ, Oosterhuis JW, Serruys PW, van der Steen A. Atherosclerotic tissue characterization *in vivo* by optical coherence tomography attenuation imaging. *J Biomed Opt* 2010;**15**:011105.
28. Sotomi Y, Onuma Y, Collet C, Tenekecioglu E, Virmani R, Kleiman NS, Serruys PW. Bioresorbable scaffold the emerging reality and future directions. *Circ Res* 2017;**120**:1341–1352.
29. Cassese S, Byrne RA, Ndrepepa G, Kufner S, Wiebe J, Repp J, Schunkert H, Fusaro M. Everolimus-eluting bioresorbable vascular scaff olds versus everolimus-eluting metallic stents: a meta-analysis of. *Lancet* 2015;**6736**:1–8.
30. Ali ZA, Serruys PW, Kimura T, Gao R, Ellis SG, Kereiakes DJ, Onuma Y, Simonton C, Zhang Z, Stone GW. 2-year outcomes with the Absorb bioresorbable scaffold for treatment of coronary artery disease: a systematic review and meta-analysis of seven randomised trials with an individual patient data substudy. *Lancet* 2017;**390**:760–772.
31. Ali ZA, Gao R, Kimura T, Onuma Y, Kereiakes DJ, Ellis SG, Chevalier B, Vu MT, Zhang Z, Simonton CA, Serruys PW, Stone GW. Three-year

outcomes with the absorb bioresorbable scaffold. *Circulation* 2018; **137**:464–479.
32. Neumann F-J, Sousa-Uva M, Ahlsson A, Alfonso F, Banning AP, Benedetto U, Byrne RA, Collet J-P, Falk V, Head SJ, Jüni P, Kastrati A, Koller A, Kristensen SD, Niebauer J, Richter DJ, Seferović PM, Sibbing D, Stefanini GG. 2018 ESC/EACTS Guidelines on myocardial revascularization. *Eur Heart J* 2018;**46**:517–592.
33. Puricel S, Cuculi F, Weissner M, Schmermund A, Jamshidi P, Nyffenegger T, Binder H, Eggebrecht H, Münzel T, Cook S, Gori T. Bioresorbable coronary scaffold thrombosis: multicenter comprehensive analysis of clinical presentation, mechanisms, and predictors. *J Am Coll Cardiol* 2016;**67**:921–931.
34. Yamaji K, Ueki Y, Souteyrand G, Daemen J, Wiebe J, Nef H, Adriaenssens T, Loh JP, Lattuca B, Wykrzykowska JJ, Gomez-Lara J, Timmers L, Motreff P, Hoppmann P, Abdel-Wahab M, Byrne RA, Meincke F, Boeder N, Honton B, OSullivan CJ, Ielasi A, Delarche N, Christ G, Lee JKT, Lee M, Amabile N, Karagiannis A, Windecker S, Räber L. Mechanisms of very late bioresorbable scaffold thrombosis: the INVEST registry. *J Am Coll Cardiol* 2017;**70**:2330–2344.
35. Onuma Y, Serruys PW. Rather thick, yet antithrombogenic: is the Magmaris scaffold a new hope for bioresorbable coronary scaffold? *Circ Cardiovasc Interv* 2017;**10**:doi:10.1161/CIRCINTERVENTIONS.117.005663.
36. Waksman R, Zumstein P, Pritsch M, Wittchow E, Haude M, Lapointe-Corriveau C, Leclerc G, Joner M. Second-generation magnesium scaffold Magmaris: device design and preclinical evaluation in a porcine coronary artery model. *EuroIntervention* 2017;**13**:440–449.
37. Bangalore S, Bezerra HG, Rizik DG, Armstrong EJ, Samuels B, Naidu SS, Grines CL, Foster MT, Choi JW, Bertolet BD, Shah AP, Torguson R, Avula SB, Wang JC, Zidar JP, Maksoud A, Kalyanasundaram A, Yakubov SJ, Chehab BM, Spaedy AJ, Potluri SP, Caputo RP, Kondur A, Merritt RF, Kaki A, Quesada R, Parikh MA, Toma C, Matar F, DeGregorio J, Nicholson W, Batchelor W, Gollapudi R, Korngold E, Sumar R, Chrysant GS, Li J, Gordon JB, Dave RM, Attizzani GF, Stys TP, Gigliotti OS, Murphy BE, Ellis SG, Waksman R. The state of the absorb bioresorbable scaffold: consensus from an expert panel. *JACC Cardiovasc Interv* 2017;**10**:2349–2359.
38. Lipinski MJ, Acampado E, Cheng Q, Adams L, Torii S, Gai J, Torguson R, Hellinga DG, Joner M, Harder C, Zumstein P, Finn AV, Kolodgie FD, Virmani R, Waksman R. Comparison of acute thrombogenicity for magnesium versus stainless steel stents in a porcine arteriovenous shunt model. *EuroIntervention* 2019;**14**:1420–1427.
39. Joner M, Ruppelt P, Zumstein P, Lapointe-Corriveau C, Leclerc G, Bulin A, Castellanos MI, Wittchow E, Haude M, Waksman R. Preclinical evaluation of degradation kinetics and elemental mapping of first- and second-generation bioresorbable magnesium scaffolds. *EuroIntervention* 2018;**14**:e1040–e1048.
40. Waksman R, Lipinski MJ, Acampado E, Cheng Q, Adams L, Torii S, Gai J, Torguson R, Hellinga DM, Westman PC, Joner M, Zumstein P, Kolodgie FD, Virmani R. Comparison of acute thrombogenicity for metallic and polymeric bioabsorbable scaffolds: magmaris versus absorb in a porcine arteriovenous shunt model. *Circ Cardiovasc Interv* 2017;**10**:e004762.
41. Otsuka F, Pacheco E, Perkins LEL, Lane JP, Wang Q, Kamberi M, Frie M, Wang J, Sakakura K, Yahagi K, Ladich E, Rapoza RJ, Kolodgie FD, Virmani R. Long-term safety of an everolimus-eluting bioresorbable vascular scaffold and the cobalt-chromium XIENCE v stent in a porcine coronary artery model. *Circ Cardiovasc Interv* 2014;**7**:330–342.
42. Verheye S, Wlodarczak A, Montorsi P, Bennett J, Torzewski J, Haude M, Vrolix M, Buck T, Aminian A, Van Der Schaaf RJ, Amin Nuruddin A, Michael Lee KY. Safety and performance of a resorbable magnesium scaffold under real-world conditions: 12-month outcomes of the first 400 patients enrolled in the BIOSOLVE-IV registry. *EuroIntervention* 2019;doi:10.4244/EIJ-D-18-01058.
43. Haude M, Ince H, Tölg R, Lemos PA, von Birgelen C, Christiansen EH, Wijns W, Neumann F-J, Eeckhout E, Garcia-Garcia HM, Waksman R. Sustained safety and performance of the second-generation drug-eluting absorbable metal scaffold (DREAMS 2G) in patients with *de novo* coronary lesions: 3-year clinical results and angiographic findings of the BIOSOLVE-II first-in-man trial. *EuroIntervention* 2019;doi:10.4244/EIJ-D-18-01000.
44. Haude M, Ince H, Kische S, Abizaid A, Tölg R, Alves Lemos P, Van Mieghem NM, Verheye S, von Birgelen C, Christiansen EH, Barbato E, Garcia-Garcia HM, Waksman R; on behalf of the BIOSOLVE-II and III investigators. Safety and clinical performance of a drug eluting absorbable metal scaffold in the treatment of subjects with *de novo* lesions in native coronary arteries: pooled 12-month outcomes of BIOSOLVE-II and BIOSOLVE-III. *Catheter Cardiovasc Interv* 2018; **92**:E502–E511.
45. Haude M, Ince H, Kische S, Abizaid A, Tölg R, Alves Lemos P, Van Mieghem NM, Verheye S, von Birgelen C, Christiansen EH, Wijns W, Garcia-Garcia HM, Waksman R. Sustained safety and clinical performance of a drug-eluting absorbable metal scaffold up to 24 months: pooled outcomes of BIOSOLVE-II and BIOSOLVE-III. *EuroIntervention* 2017;**13**:432–439.
46. Kandzari DE, Koolen JJ, Doros G, Massaro JJ, Garcia-Garcia HM, Bennett J, Roguin A, Gharib EG, Cutlip DE, Waksman R. Ultrathin bioresorbable polymer sirolimus-eluting stents versus thin durable polymer everolimus-eluting stents. *J Am Coll Cardiol* 2018;**72**:3287–3297.
47. Colleran R, Bch MB, Joner M, München DH, München TU, German D. The COMBO stent: can it deliver on its dual promise? *AsiaIntervention* 2017;**3**:15–17.
48. Bourantas CV, Jaffer FA, Gijsen FJ, Van Soest G, Madden SP, Courtney BK, Fard AM, Tenekecioglu E, Zeng Y, Van Der Steen AFW, Emelianov S, Muller J, Stone PH, Marcu L, Tearney GJ, Serruys PW. Hybrid intravascular imaging: recent advances, technical considerations, and current applications in the study of plaque pathophysiology. *Eur Heart J* 2017;**38**:400–412b.
49. Joner M, Giacoppo D, Kastrati A. Molecular multimodality imaging: has a long-standing dream come true? *Eur Heart J* 2017;**38**:456–458.
50. Tarkin JM, Dweck MR, Evans NR, Takx RAP, Brown AJ, Tawakol A, Fayad ZA, Rudd J. Imaging atherosclerosis. *Circ Res* 2016;**118**:750–769.